Boundary conformal field theories and loop models

2009 J. Phys. A: Math. Theor. 42 345004

(http://iopscience.iop.org/1751-8121/42/34/345004)

IOP PUBLISHING JOURNAL OF PHYSICS A: MATHEMATICAL AND THEORETICAL

J. Phys. A: Math. Theor. **42** (2009) 345004 (16pp) doi:10.1088/1751-8113/42/34/345004

Boundary conformal field theories and loop models

M A Rajabpour

Dipartimento di Fisica Teorica and INFN, Università di Torino, Via P Giuria 1, 10125 Torino, Italy and
Institute for Studies in Theoretical Physics and Mathematics, Tehran 19395-5531, Iran

E-mail: rajabpour@to.infn.it

Received 27 May 2009, in final form 12 July 2009
Published 6 August 2009
Online at stacks.iop.org/JPhysA/42/345004

Abstract

We propose a systematic method to extract conformal loop models for rational conformal field theories (CFT). The method is based on defining an ADE model for boundary primary operators by using the fusion matrices of these operators as adjacency matrices. These loop models respect the conformal boundary conditions. We discuss the loop models that can be extracted by this method for minimal CFTs and then we give dilute $O(n)$ loop models on the square lattice as examples for these loop models. We also give some proposals for WZW $SU(2)$ models.

PACS numbers: 05.50.+q, 11.25.Hf, 05.10.Gg

1. Introduction

The study of statistical models related to loop models is interesting both from the physical and mathematical points of view. Most of the statistical models studied in physics such as the Ising, the q-state Potts model and also complicated vertex models can be represented in terms of loops [1]. The loop representation of the spin system is very easy to understand: loops correspond to domain walls separating regions of different magnetization. The study of critical loop models can be interesting from many points of view: they are good candidates for the ground state of topological quantum systems [2]; they are also lattice models for the Schramm–Loewner evolution (SLE), a method discovered by Schramm [3] to classify conformally invariant curves connecting two distinct boundary points in a simply connected domain.

Different applications of conformal loop models stimulate a systematic study of these models by conformal field theory (CFT). Recently, we proposed in [4] a method to extract loop models corresponding to a conformal field theory. The method was based on defining an RSOS model for every primary operator by using the fusion matrix of the primary operator as an adjacency matrix and then extracting the loop model corresponding to domain walls of the

RSOS model. The fugacity of a loop is equal to the quantum dimension of the corresponding operator. This method is in close relation with Pasquier's classification of ADE lattice models and their loop representations [5]. In this paper, we want to follow the same method consistent with the conformal boundary operators. Since SLE is a boundary CFT we think that using the fusion matrix of boundary operators as an adjacency matrix is more consistent with the nature of SLE. Recently, a very nice and extensive project was initiated by Jacobsen and Saleur [6] followed by Dubail *et al* [7, 8] to classify all the possible conformal boundary loop models. It is based on classifying the possible boundary loop models compatible with the boundary conformal field theories. This classification is in close relation with the earlier work by Cardy on formulating the modular invariant partition function of the $O(n)$ model on the annulus [9]. The results that we get by our method apart from simplicity are all compatible with the results in [6, 7, 9].

The paper is organized as follows. In the following section, we will introduce the necessary ingredients to find the boundary operators and also the fusion matrices corresponding to them. In the third section, we briefly review the method proposed in [4] and we will also generalize it to the graphs with largest eigenvalue greater than 2. The central claim of this section is as follows: the loop model extracted with this method is connected with the properties of the statistical loop model in the same universality class as the corresponding CFT. In the third section, we follow explicitly some examples, in particular, the Ising model, the tri-critical Ising model, the three-state Potts model and the tri-critical three-state Potts model. Then we give the possible loop models, extractable with this method, of minimal CFTs and also the lattice models corresponding to these loop models. We close this section by giving some proposals for possible loop models for WZW $SU(2)$ models. The last section contains our conclusions with a brief description of the work in progress motivated by these results.

2. Boundary conformal field theory

To define the loop model for a generic minimal CFT consistent with the conformal boundary we need to first summarize the main important facts about boundary CFT. The most important ingredient to classify the boundary conformal operators is the modular invariant partition function of the CFT. The classification of modular invariant partition functions of $SU(2)$ minimal models is well known and can be related to a pair of simply laced Dynkin diagrams (A, G) [10]. The complete classification based on ADE diagrams is

$$(A, G) = \begin{cases} (A_{h-1}, A_{g-1}) & \\ (A_{h-1}, D_{(g+2)/2}), & g \text{ even} \\ (A_{h-1}, E_6), & g = 12 \\ (A_{h-1}, E_7), & g = 18 \\ (A_{h-1}, E_8), & g = 30, \end{cases} \tag{2.1}$$

where g and h are the Coxeter numbers of A and G with $h, g \geqslant 2$. The above pair of Dynkin diagrams describes the bulk modular invariant partition function with some primary operators and with the following central charge:

$$c = 1 - 6\frac{(h-g)^2}{hg}. \tag{2.2}$$

Each of the unitary minimal models $M(A_{h-1}, G)$ with $g - h = \pm 1$ can be realized as the continuum scaling limit of an integrable two-dimensional lattice model at criticality, with heights living on the nodes of the graph G. In particular, the critical series with $g - h = 1$ is associated with the A–D–E lattice models [11]. The tri-critical series with $g - h = -1$ is

Table 1. The Coxeter number and the Coxeter exponents of Dynkin diagrams.

Dynkin diagram	Coxeter number (h)	Coxeter exponent (m)
A_n	$n+1$	$1, 2, \ldots, n$
D_n	$2(n+1)$	$1, 3, \ldots, 2n-1, n-1$
E_6	12	1, 4, 5, 7, 8, 11
E_7	18	1, 5, 7, 9, 11, 13, 17
E_8	30	1, 7, 11, 13, 17, 19, 23, 29

associated with the dilute lattice models [12, 13]. For theories with a diagonal torus partition function it is known that there is a conformal boundary condition associated with each operator in the theory [14]. The fusion rules of these boundary operators are just given by the bulk fusion algebra. It was shown in a series of papers that for $SU(2)$ minimal models one can propose a complete set of conformal boundary operators $i = (r, a) \in (A, G)$, where r and a are nodes on the Dynkin diagram of A and G, respectively. There is the identification $(r, a) = (h - r, \gamma(a))$, where γ is an automorphism acting on the nodes of the graph G. This automorphism is identity except for the A, E_6 and D_{odd} which is the Z_2 symmetry of the Dynkin diagram. Symmetries of Dynkin diagrams play an important rule in the forthcoming discussion. Following [15] we show the corresponding operators by $\hat{\phi}_i$ and the independent boundary states by $|(r, a)\rangle$ which is called Cardy states. Cardy states can be written in terms of Ishibashi states, i.e. $|j\rangle\rangle$, as follows $|(r, a)\rangle = \sum_j c^j_{(r,a)}|j\rangle\rangle$, where the sum is over all Ishibashi states. We are interested in the fusion rules of these boundary operators. To give a formula for the fusion rules of these operators we need to define some quantities. Let Ψ be the eigenvectors of the adjacency matrix corresponding to the group G. Then the graph fusion matrices $\hat{N}_a$ with $a \in G$ can be defined as follows:

$$(\hat{N}_a)_b{}^c = \sum_{m \in \text{Exp}(G)} \frac{\Psi_{\text{am}} \Psi_{\text{bm}} \Psi^*_{\text{cm}}}{\Psi_{1\text{m}}}, \qquad a, b, c \in G, \tag{2.3}$$

where $\text{Exp}(G)$ denotes the set of exponents of G, see table 1. Let us show also the graph fusion matrix for A_{h-1} by N_r then following [15] the fusion rules for boundary operators are

$$\hat{\phi}_{i_1} \hat{\phi}_{i_2} = \sum_{i_3 \in (A,G)} \left(\mathcal{N}_{i_1}\right)^{i_3}_{i_2} \hat{\phi}_{i_3}, \tag{2.4}$$

where $(\mathcal{N}_{i_1})^{i_3}_{i_2}$ has the following relation with the graph fusion matrices of A and G:

$$\left(\mathcal{N}_{(r_1,a_1)}\right)^{(r_3,a_3)}_{(r_2,a_2)} = N^{r_3}_{r_1 r_2} \hat{N}^{a_3}_{a_1 a_2}. \tag{2.5}$$

For more details about the connection of the boundary operators to bulk counterparts see [15, 16].

To calculate the fusion matrices of boundary operators we also need to define a conjugation operator $C(a) = a^*$. It is the identity except for D_{4n} graphs where the eigenvectors Ψ_{am} are complex and conjugation corresponds to the Z_2 Dynkin diagram automorphism. It then follows that $\hat{N}^c_{a^* b} = \hat{N}^b_{ca}$. The operator $C(a)$ acts on the right to raise and lower indices in the fusion matrices $\hat{N}^a = \hat{N}_a C$. It is an important ingredient to get the right fusion matrices for the boundary operators, in particular for the D_{4n} graphs. We will give some examples in section 4, in particular, we use the above method to get the fusion matrices of the boundary operators of the Ising model, the tri-critical Ising model, the three-state Potts model and the tri-critical three-state Potts model.

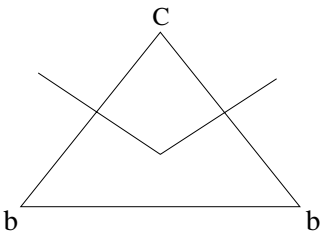

Figure 1. A triangular plaquette with $c \neq b$ and the corresponding curve segment on the dual honeycomb lattice.

3. Loop models for boundary operators

In this section, we propose a method to extract some possible loop models for CFTs; the method is the same as the method introduced recently in [4]. In this reference, we showed that using the fusion matrix as an adjacency matrix it is possible to associate a $O(n)$ loop model with every primary operator. The method is described briefly as follows: the graph of a primary operator $\hat{\phi}_i$ has g vertices, where g is the number of primary operators in the theory and edges connecting pairs of vertices (j, k) when $\mathcal{N}_{ij}^k = 1$. Following [26] one can define a height model on the triangular lattice by imposing that the height h_j at the site j can take values $0, 1, \ldots, g-1$. Then constraint the heights at neighboring sites according to the incidence matrix associated with a given primary field $\hat{\phi}_i$. Only neighbor heights h_j and h_k with $(\mathcal{N}_i)_j^k = 1$ are admissible. For a consistent definition of loop models on a triangular lattice at least two of the heights at the corners of an elementary triangular plaquette should be equal. Then the weights for the elementary plaquette are defined as follows: if the heights of the plaquette are (c, b, b) with $c \neq b$ then the weight is $x\left(\frac{\hat{S}_l^b}{\hat{S}_l^c}\right)^{1/6}$, where $\hat{S}$ satisfies $\sum_b (\mathcal{N}_a)_b^c \frac{\hat{S}_l^b}{\hat{S}_l^0} = \frac{\hat{S}_l^a}{\hat{S}_0^l}\frac{\hat{S}_l^c}{\hat{S}_l^0}$. It means that the bth element of the eigenvector of $\mathcal{N}_a$ with eigenvalue $\frac{\hat{S}_l^a}{\hat{S}_0^l}$ is given by $\frac{\hat{S}_l^b}{\hat{S}_l^0}$. If the heights are all equal then the weight is 1 except for those with $\mathcal{N}_{ab}^b \neq 0$ that have weights 1 or x depending on the particular model considered[1]. The next step is to mark triangles with unequal heights (c, b, b) drawing a curved segment on the dual honeycomb lattice [26] and linking to the center the midpoints of the two edges with different heights (b and c) at the extremes (see figure 1). Summing over the admissible values of heights consistent with a given loop configuration we find

$$\sum_b (\mathcal{N}_a)_b^c \frac{\hat{S}_l^b}{\hat{S}_l^c} = \frac{\hat{S}_l^a}{\hat{S}_0^l}, \tag{3.1}$$

where the sum is just over b. We take most of the times $l = 0$ to get the largest eigenvalue of $\mathcal{N}_a$ to guarantee positive real weights in our height models, however, we will also point to other cases. The fugacity of loops is given by the largest eigenvalue of the fusion matrix n_a. The partition function of the model is as follows:

$$Z = \sum x^l n_a^N, \tag{3.2}$$

where l is the number of bonds in the loop configuration and N is the number of loops. Using this method we can correspond to every boundary conformal operator a $O(n)$ loop model.

[1] For more details especially about identical neighbor heights see [4].

Since the $O(n)$ model possesses a dilute critical point for $n \leqslant 2$ with $x_c = \frac{1}{\sqrt{2+\sqrt{2-n}}}$; see [17], correspondingly our loop models will have a critical point just for the fields with n_a less than 2. The $O(n)$ model has another critical regime, the so-called dense phase, for $x = (x_c, \infty)$ which corresponds to a different universality class. Mapping to the $O(n)$ model helps us to find the connection with SLE: from Coulomb gas arguments we know that, in the dilute regime, the loop weight has the following relation with the drift in the SLE equation

$$n_a = -2\cos\left(\frac{4\pi}{\kappa}\right). \tag{3.3}$$

For the dense phase the above equation is still true if we work in the region $4 \leqslant \kappa \leqslant 8$. Using the above equation we can find the properties of the loop model corresponding to a boundary conformal operator. The achievement of this method respects the Cardy's equation [14]: *fields in the same sector have the same loop representation*.

Before generalizing the definition to more general graphs we should stress that although we started with well-defined minimal CFT the loop model that we extracted is not necessarily minimal. The point is that the extracted loop model respects some aspects of the corresponding conformal field theory. This is akin to saying that although the domain walls in the Ising model at the critical point are the same as the critical $O(n = 1)$, the Ising conformal field theory does not explain all the aspects of the critical curves. From this point the loop model that one can get by this method from the rational CFT is not perfectly equal to the corresponding CFT.

One can generalize the above idea to the decomposable fusion graphs by the method that was explained in [18]. Since the fusion graphs of some operators in minimal models are equivalent to the tensor product of two adjacency diagrams, one can use this method to extract new loop models that can also have configurations with crossing loop segments. The general strategy is based on extracting critical loop models with $n \leqslant 2$ for the graphs with largest eigenvalue greater than 2. Some graphs obey simple decomposition, and can be written as a tensor product, but others need to be mapped to simple decomposable graphs by going to the ground-state adjacency graph [18]. Here we just comment on decomposable graphs $\mathcal{N} = \mathcal{N}_1 \otimes \mathcal{N}_1$, where $\mathcal{N}_1$ and $\mathcal{N}_2$ are simple ADE diagrams. In these cases, we can define the two-flavor loop model living on the honeycomb lattice independently: one is related to the loop model of $\mathcal{N}_1$ with fugacity n_1 and the other comes from the graph $\mathcal{N}_2$ with fugacity n_2. Fendley showed [18] that in this case it is also possible to define consistently interacting loop models on the square lattice with partition function $Z = \sum n_1^{N_1} n_2^{N_2} b^C$, where $N_{1,2}$ are the numbers of each kind of loop and C is the number of plaquettes with a resolved potential crossing at their center. The critical values of b were calculated in [19] but the critical properties of the loops are still unsolved. This is obviously not the only method to define the loop model for non-simple graphs; another method is based on the multi-flavor loop model of [13]. In these models, a curve of flavor i separating two neighboring sites does not necessarily separate two sites with different heights; for the definition of the RSOS model in this case and its relation to the loop model see [13].

In the following section, we summarize some simple examples including the most familiar minimal conformal models such as Ising, tri-critical Ising, three-state Potts model and tri-critical three-state Potts model. The main point is to take the fusion graphs as adjacency graphs in the consistent way and to extract some loop models. These loop models are not equivalent to the corresponding conformal field theory, but still carry some aspects of the underlying field theory in a consistent way. In particular, the critical properties of these loop models are in close connection with the corresponding conformal field theory.

In this paper, some distinctions are crucial. We have some minimal conformal field theories with well-defined fusion matrices and modular invariant partition functions; one

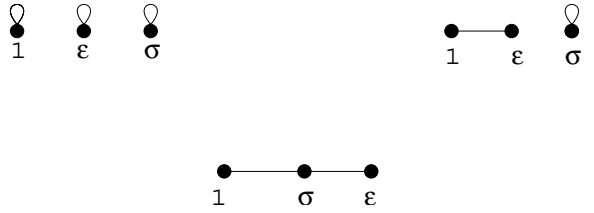

Figure 2. Graphs of fusion matrices of boundary primary operators in the Ising model, from the left to the right the fusion graphs of 1, ϵ and σ. The graph of the operator ϵ is A_2 and the graph of σ is A_3.

example is Ising conformal field theory. There are some statistical models such as spin models, RSOS models which at the critical point can be described partially by the minimal CFT, so the Ising CFT is different from the statistical Ising model. We prefer also to distinguish between for example the dilute ADE models and the dilute $O(n)$ loop model. They can be mapped to each other and have the same phase transitions but since the fundamental object in one side is local and in the other one is non-local this distinction is useful. Much work has been done on connecting these two models, minimal conformal field theories and statistical models counterparts, using integrability methods. Our argument hardly has something new to say from this point of view. Finally, we define another statistical model by using the fusion matrices of primary operators of conformal field theory which most of the time is in the same universality class as the statistical model counterpart of the corresponding CFT. These height models also have loop representations. This similarity can be useful to get an idea about the loop properties of the statistical models with well-known minimal CFTs.

4. Some examples

In this section, we apply the method introduced in section 3 to the minimal conformal field theories with the well-defined fusion structure and also WZW $SU_k(2)$ models. We will also comment on the consistency of these loop models with the Cardy's boundary states. This consistency is a hint to believe that it may be possible to extend the results into the level of the boundary partition function [9]. For notational convenience in this section of the paper we will drop the hat of boundary operators.

4.1. Ising model

The simplest example is the Ising model (A_2, A_3). Since the model has the diagonal modular invariant partition function the fusion matrices of the boundary operators are the same as the bulk case. The fusion graphs are as in figure 2 so the boundary states are as follows:

$$\begin{aligned}
|\mathbf{1}\rangle &= \frac{1}{\sqrt{2}}|\mathbf{1}\rangle\rangle + \frac{1}{\sqrt{2}}|\epsilon\rangle\rangle + \frac{1}{\sqrt[4]{2}}|\sigma\rangle\rangle,\\
|\epsilon\rangle &= \frac{1}{\sqrt{2}}|\mathbf{1}\rangle\rangle + \frac{1}{\sqrt{2}}|\epsilon\rangle\rangle - \frac{1}{\sqrt[4]{2}}|\sigma\rangle\rangle,\\
|\sigma\rangle &= |\mathbf{1}\rangle\rangle - |\epsilon\rangle\rangle.
\end{aligned} \tag{4.4}$$

These equations reflect the Z_2 symmetry corresponding to changing the sign of the spin, this is also evident in the loop representation; $n_\epsilon = n_{\mathbf{1}} = 1$. Both operators give $\kappa = 3$; these loops are the domain walls between different spins. It is worth mentioning that this symmetry comes from the natural Z_2 symmetry of the Dynkin diagram. The operator σ with

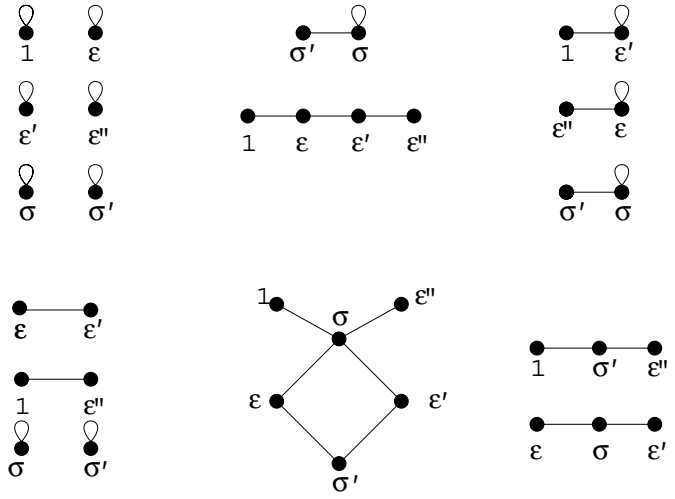

Figure 3. Graphs of fusion matrices of the boundary primary operators in the tri-critical Ising model. In the upper row from left to right are the fusion graphs of 1, ϵ and ϵ'; in the lower row from left to right are the fusion graphs of ϵ''; σ and σ'. The fusion graph of ϵ is A_4 plus T_2; they are connected to each other by folding duality. The fusion graph of σ is $T_2 \otimes A_3$.

$n_\sigma = \sqrt{2}$ corresponds to the free boundary condition. A loop in the dense phase has $\kappa = \frac{16}{3}$ and describes the domain walls of Fortuin–Kasteleyn (FK) clusters. In the above calculation we considered only the largest eigenvalue of the fusion graphs; however, it is also possible to consider other eigenvalues as the fugacity of the loop, and the cost accepts complex local Boltzmann weights for the corresponding height model. Since loop models are generically non-local theories, accepting complex Boltzmann weights for the height models (most of the time) is equal to accepting non-unitary theories. By this introduction one can accept the possibility of loop models with $n = \pm\sqrt{2}, 0$ for the loop models corresponding to the A_3 diagram of the spin operator.

4.2. Tri-critical Ising model

The next simple example is the tri-critical Ising model, (A_3, A_4) which has diagonal modular invariant partition function. The boundary CFT of this model was discussed in [20]. There are six boundary operators $\mathbf{1}, \epsilon, \epsilon', \epsilon'', \sigma$ and σ' with the fusion graphs as in figure 3 and the following Cardy states

$$
\begin{aligned}
|\mathbf{1}\rangle &= C[|\mathbf{1}\rangle\rangle + \eta|\epsilon\rangle\rangle + \eta|\epsilon'\rangle\rangle + |\epsilon''\rangle\rangle + \sqrt[4]{2}|\sigma'\rangle\rangle + \sqrt[4]{2}|\sigma\rangle\rangle],\\
|\epsilon\rangle &= C[\eta^2|\mathbf{1}\rangle\rangle - \eta^{-1}|\epsilon\rangle\rangle - \eta^{-1}|\epsilon'\rangle\rangle + \eta^2|\epsilon''\rangle\rangle - \sqrt[4]{2}\eta^2|\sigma'\rangle\rangle + \sqrt[4]{2}\eta^{-1}|\sigma\rangle\rangle],\\
|\epsilon'\rangle &= C[\eta^2|\mathbf{1}\rangle\rangle - \eta^{-1}|\epsilon\rangle\rangle - \eta^{-1}|\epsilon'\rangle\rangle + \eta^2|\epsilon''\rangle\rangle + \sqrt[4]{2}\eta^2|\sigma'\rangle\rangle - \sqrt[4]{2}\eta^{-1}|\sigma\rangle\rangle],\\
|\epsilon''\rangle &= C[|\mathbf{1}\rangle\rangle + \eta|\epsilon\rangle\rangle + \eta|\epsilon'\rangle\rangle + |\epsilon''\rangle\rangle - \sqrt[4]{2}|\sigma'\rangle\rangle - \sqrt[4]{2}|\sigma\rangle\rangle],\\
|\sigma'\rangle &= \sqrt{2}C[|\mathbf{1}\rangle\rangle - \eta|\epsilon\rangle\rangle + \eta|\epsilon'\rangle\rangle - |\epsilon''\rangle\rangle],\\
|\sigma\rangle &= \sqrt{2}C[\eta^2|\mathbf{1}\rangle\rangle + \eta^{-1}|\epsilon\rangle\rangle - \eta^{-1}|\epsilon'\rangle\rangle - \eta^2|\epsilon''\rangle\rangle],
\end{aligned}
\tag{4.5}
$$

where $C = \sqrt{\frac{\sin\frac{\pi}{5}}{\sqrt{5}}}$ and $\eta = \sqrt{2\cos\frac{\pi}{5}}$. The boundary states corresponding to boundary operators $\mathbf{1}$ and ϵ'' can be transformed to each other by just changing the sign of spin operators, i.e. Z_2 symmetry. They have also the same loop weight $n = 1$ that comes from the largest

eigenvalue of the fusion matrix[2]. The boundary states ϵ and ϵ' are connected also by just changing the sign of the spin states. The weight of the loops is $n = 2\cos(\frac{\pi}{5})$ with $\kappa = 5$ in the dense phase. This loop model corresponds to the boundary of geometric clusters at the geometric critical point of the tri-critical Ising model or the Blume–Capel model [22]. The operator σ' describes a loop model with $n = \sqrt{2}$. The loop model has $\kappa = \frac{16}{5}$ in the dense phase which is related to the boundary of spin clusters and also vacancy clusters in the Blume–Capel model [22, 23]. The interesting point for tri-critical models is the equality of critical exponents for spin clusters and FK clusters [22, 23]. The operator σ is related to the degenerate boundary condition and the corresponding loop model with $n = 2\sqrt{2}\cos(\frac{\pi}{5})$ is non-critical. However, it is easy to see that the fusion matrix of this operator is decomposable to simple matrices $N_\sigma = N_{T_2} \otimes N_{A_3}$. Then for this graph we have two-flavor loop model with fugacities $n_1 = \sqrt{2}$ and $n_2 = 2\cos\left(\frac{\pi}{5}\right)$. One can conclude from the above discussion that those operators with the same loop representations are connected to each other by folding and orbifold duality and it is also possible to see these symmetries in the level of boundary states.

Similar to the previous subsection one can also consider that other possible loop weights come from the other eigenvalues of the fusion matrix. The eigenvalues of the fusion matrix of the operator ϵ are $n = \pm 2\cos\left(\frac{\pi}{5}\right), \pm\frac{1}{2\cos(\frac{\pi}{5})}$ and the eigenvalues of the fusion matrix of the operator σ' are $\pm\sqrt{2}, 0$. The eigenvalues of the other operators are a subset of the above eigenvalues. Interestingly, apart from the negative eigenvalues, the above numbers can be fitted with the boundary loop weights in both dense [6–8] and dilute [8] regimes[3]. However, the height models in these cases have negative Boltzmann weights and so are obviously non-unitary but in the level of loop model one can think about the unitary loop model. In other words, two different Boltzmann weights, one real and the other complex, can give similar loop models. However, in our calculation the criterion for the existence of real Boltzmann weights is not obvious and needs more investigation.

4.3. Three-state Potts model

The next example is the first non-diagonal case, the three-state Potts model (A_4, D_4) with eight boundary operators $\mathbf{1}, \psi, \psi^\dagger, \epsilon, \sigma, \sigma^\dagger, \phi_{1,2}$ and $\hat{\phi}_{2,2}$, see [14, 15, 24]. The fusion graphs are given in figure 4. Following Cardy's argument one can show that the operators $\mathbf{1}, \psi, \psi^\dagger$ correspond to fix boundary conditions and the corresponding boundary states can be transformed to each other by the Z_3 symmetry, i.e. the symmetry of the Dynkin diagram D_4. They also have the same quantum dimensions $n_{\mathbf{1}} = n_\psi = n_{\psi^\dagger} = 1$. The operators $\epsilon, \sigma, \sigma^\dagger$ describe the fluctuating boundary conditions [25] and all have the same kinds of fusion graphs with $n_\epsilon = n_\sigma = n_{\sigma^\dagger} = 2\cos(\frac{\pi}{5})$. In the dilute phase one can consider $\kappa = \frac{10}{3}$ as a SLE drift. In the lattice three-state Potts model, these loops are the same as the domain walls between one definite spin cluster with the other two spins [25]. The fusion graph of the operator $\phi_{1,2}$ is two D_4 graphs. This operator describes the fix boundary condition and has the loop model with $n = \sqrt{3}$ which is equal to the fugacity of domain walls in FK clusters of the three-state Potts model. The operator $\phi_{2,2}$ describes the degenerate boundary condition and the corresponding loop model with $n_{\phi_{2,2}} = \sqrt{\frac{9+3\sqrt{5}}{2}}$ is non-critical; however, decomposition is possible. In this case, one can write $N_{\phi_{2,2}} = N_{T_2} \otimes N_{D_4}$ and so the corresponding two-flavor loop model has fugacities $n_1 = \sqrt{3}$ and $n_2 = 2\cos\left(\frac{\pi}{5}\right)$.

[2] To get the loop weights we consider one simply connected part of the fusion graph as an adjacency graph; the other parts of the graph have always equal largest eigenvalues. One can see that these different parts are folding or orbifold dual of each other, see [21].

[3] The consistency is just at the level of integer r mentioned in [7, 8].

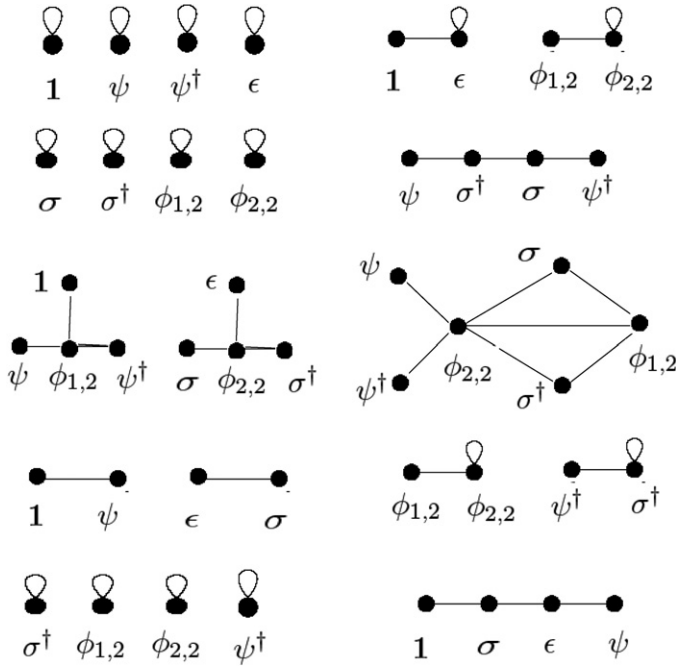

Figure 4. Graphs of fusion matrices of primary operators in the three-state Potts model. In the upper row from left to right are the fusion graphs of 1 and ϵ; in the middle row from left to right are the fusion graphs of $\phi_{1,2}$ and $\phi_{2,2}$ and in the lowest row are the fusion graphs of ψ and σ. The fusion graphs of $\psi^\dagger$ and $\sigma^\dagger$ can be derived from the fusion graphs of ψ and σ by the following exchanges: $\psi \leftrightarrow \psi^\dagger$ and $\sigma \leftrightarrow \sigma^\dagger$. The fusion graph of ϵ is A_4 plus two T_2 graphs, they are connected to each other by folding duality. The fusion graph of $\phi_{1,2}$ is two D_4 and the fusion graph of $\phi_{2,2}$ is $T_2 \otimes D_4$.

The fusion matrix of ϵ as was discussed in the case of the tri-critical Ising model has eigenvalues $n = \pm 2\cos\left(\frac{\pi}{5}\right), \pm\frac{1}{2\cos(\frac{\pi}{5})}$. The eigenvalues of N_{D_4} are $\pm\sqrt{3}, 0$. These loop weights can be fitted with the boundary loop fugacities in [6–8].

4.4. Tri-critical three-state Potts model

The next interesting example is the tri-critical three-state Potts model (D_4, A_6). It has the non-diagonal modular invariant partition function and also it is not part of Pasquirer's A–D–E models. The boundary states of this model have not been investigated systematically so far. The boundary operators of this model are ϕ_i with $i = (r, a)$, $r = 1, 2, 3$ and $a = 1, \ldots, 4$. The fusion graphs for the boundary operators in this case are given in the appendix. The boundary states corresponding to boundary operators $\phi_{1,1}, \phi_{1,3}, \phi_{1,4}$ can be transformed to each other by the Z_3 symmetry of spin operators and should correspond to fix boundary conditions with $n = 1$. The operators $\phi_{2,1}, \phi_{2,3}, \phi_{2,4}$ have also the same property with the same fusion graphs with $n = 2\cos(\frac{\pi}{7})$. In the lattice tri-critical three-state Potts model, they are domain walls of geometric clusters of geometric critical point [22] with $\kappa = 4\frac{7}{6}$. The operators $\phi_{3,1}, \phi_{3,3}, \phi_{3,4}$ can be transformed to each other by the Z_3 symmetry; however, they have loop fugacities greater than 2; $n = 2.246$. The operators $\phi_{2,2}$ and $\phi_{3,2}$ have also loop weights more than 2 and are related to degenerate boundary conditions. Finally, the graph of $\phi_{1,2}$ is equal to three

D_4 graphs with $n = \sqrt{3}$. In the dilute phase, this weight describes the domain walls of spin clusters in the lattice tri-critical three-state Potts model with $\kappa = 4\frac{6}{7}$.

The fusion graph of $\phi_{2,1}$ is the sum of two graphs A_6 and T_3. The fusion matrix has the eigenvalues $n = 2\cos\left(\frac{\pi j}{7}\right)$ with $j = 2, 3, 4, 5, 6$. The eigenvalues of the fusion matrix of $\phi_{1,2}$ are $n = \pm\sqrt{3}, 0$. Interestingly, again apart from the negative eigenvalues, the above numbers can be fitted with the boundary loop weights in [6, 7]. The fusion graph of $\phi_{2,2}$ is decomposable as $T_3 \otimes D_4$ and so it is possible to define two crossing loop models in this case. The fusion graphs of $\phi_{3,1}$ are not decomposable to simple graphs so it is not possible to extract critical loops also for $\phi_{3,3}$ and $\phi_{3,4}$ which are in the same sector. Although the loops, extracted by our method, corresponding to the above operators are not critical, by considering the fusion graph of the ground state of the above adjacency graph it is possible to extract critical loops. We will not discuss this method here, for more details one can see [18]. The fusion graph of $\phi_{3,2}$ is decomposable but not to the simple graphs, i.e. $N_{\phi_{3,2}} = N_{T_3^2} \otimes N_{D_4}$. Another possibility to extract critical loops for $\phi_{3,1}$ is by considering other eigenvalues of the fusion matrix of this operator. The eigenvalues of $N_{\phi_{3,1}}$ are $\pm\frac{\sin(\frac{3\pi}{7})}{\sin(\frac{\pi}{7})}$, $\pm\frac{\sin(\frac{2\pi}{7})}{\sin(\frac{\pi}{7})}$ and $\pm\frac{\sin(\frac{\pi}{7})}{\sin(\frac{2\pi}{7})}$; the last two cases have critical loops.

4.5. Minimal models

Finding loop models by the method explained in section 3 is general and applicable for more generic cases. Take a pair (A, G) from equation (2.1); then it is possible to correspond at least two different kinds of loop models for these minimal models with the following weights:

$$n = 2\cos\left(\frac{\pi}{g}\right), \qquad n = 2\cos\left(\frac{\pi}{h}\right). \tag{4.6}$$

They are the largest eigenvalues of the fusion matrices of $\phi_{1,2}$ and $\phi_{2,1}$. One can also consider the following SLE drifts for these loop models:

$$\begin{aligned} &\kappa = 4\frac{g}{g+1}, \qquad \kappa = 4\frac{h}{h-1}, \qquad g - h = 1, \\ &\kappa = 4\frac{g}{g-1}, \qquad \kappa = 4\frac{h}{h+1}, \qquad g - h = -1. \end{aligned} \tag{4.7}$$

The other eigenvalues of G can be written as

$$n = 2\cos\left(\frac{\pi m}{g}\right), \tag{4.8}$$

where m is one of the Coexter exponents of the graph G. They are listed in table 1.

It is possible to consider loop models for the above eigenvalues as before; however, they are not still all the possible loop models. We already showed in some cases that one can define two flavor loop models for decomposable fusion graphs. It is also possible, as in the case of the fusion graph of $\phi_{3,1}$ in the tri-critical three-state Potts model, to have matrices with relevant non-largest eigenvalues. We believe that they are relevant because the same loop weights appear in the classification of Jacobsen and Saleur [6].

Although so far we have given more familiar examples as the possible candidates for our loop models, it is also possible to extract systematic examples for the above proposals by using Pasquier's ADE models and dilute ADE models [12, 13]. Pasquier's ADE models give a lattice realization for the (A, G) series with $g - h = 1$ and the description briefly is as follows: define an RSOS model by using the graph G. This height model at the critical point can be described by a minimal CFT. Then map this height model to the loop model [26] at the critical point

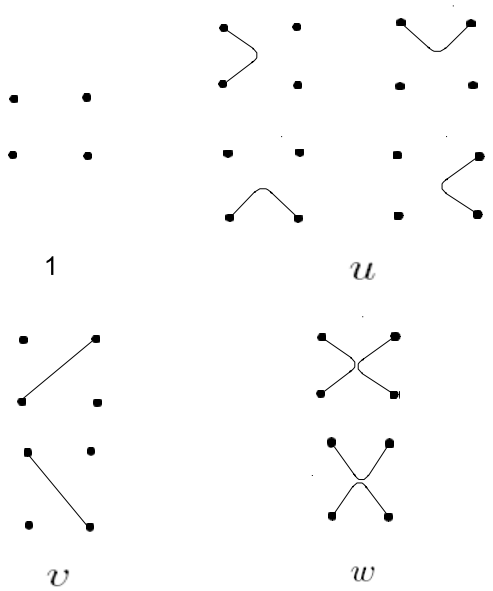

Figure 5. The Boltzmann weights of the different vertices in the $O(n)$ model on the square lattice.

with $n = 2\cos(\frac{\pi}{g})$ which is the same as the loop model that we proposed in (4.6). Of course the method proposed in this paper and [4] is highly influenced by Pasquier's ADE models but it has something more to say by connecting the loop properties to the fusion properties of the primary operators. To get the dilute loop models and the loop models corresponding to tri-critical models we need to use dilute ADE models. These models have rich phase diagrams with four branches: branches 1 and 2 have central charges $c = 1 - \frac{6}{g(g\pm1)}$ and branches 3 and 4 have $c = \frac{3}{2} - \frac{6}{g(g\pm1)}$. One can also map these height models to $O(n)$ loop models with the non-intersecting bonds on the square lattice with the partition function

$$Z = \sum u^{N_u} v^{N_v} w^{N_w} n^N, \tag{4.9}$$

where the weights for different plaquettes are given in figure 5 and N_u, N_v and N_w are the numbers of different plaquettes [27]. This generalized $O(n)$ loop model apart from the critical properties at $u = w = \frac{1}{2}$ and $v = 0$ has four other branches which coincide with the four branches of dilute ADE models [29]. The weights are given by

$$\begin{aligned} n &= -2\cos(2\theta), \\ w &= \frac{1}{2 - [1 - 2\sin(\theta/2)][1 + 2\sin(\theta/2)]^2}, \\ u &= \pm 4w \sin(\theta/2)\cos(\pi/4 - \theta/4), \\ v &= \pm w[1 + 2\sin(\theta/2)], \end{aligned} \tag{4.10}$$

where $\frac{\pi}{2} \leqslant \theta \leqslant \pi, 0 \leqslant \theta \leqslant \frac{\pi}{2}, -\frac{\pi}{2} \leqslant \theta \leqslant 0$ and $-\pi \leqslant \theta \leqslant -\frac{\pi}{2}$ are the intervals corresponding to branches 1, 2, 3 and 4, respectively. They coincide with the different branches in the dilute ADE models.

It is interesting to investigate the connection of the above loop model to the SLE. There are different methods for doing this; here we use the magnetic operator to find the SLE drift.

It was shown in [27] by numerical calculation that the magnetic exponent of the branches 1 and 2 is identified with $2h_{\frac{m+1}{2},\frac{m+1}{2}}$ where

$$h_{r,s} = \frac{((m+1)r - ms)^2 - 1}{4m(m+1)}, \tag{4.11}$$

and m is related to the central charge of the theory by $c = 1 - \frac{1}{m(m+1)}$. Its connection to the loop variables comes from the relation $\frac{2\theta}{\pi} + \frac{\pi}{2\theta} - 2 = \frac{1}{m(m+1)}$ derived from the coulomb gas method [27]. The connection of the magnetic exponent to the SLE drift is as follows [28]:

$$2h_{\frac{m+1}{2},\frac{m+1}{2}} = \frac{(8-\kappa)(3\kappa-8)}{32\kappa}. \tag{4.12}$$

Using the above equation the SLE drift at branches 1 and 2 of the loop model (4.9) can be derived as follows:

$$\kappa = \frac{8\theta}{\pi}. \tag{4.13}$$

This result is also consistent with our expectation from the second level null vector of minimal models [30], it is also consistent with the recent direct investigation by using holomorphic variables [31] .

Back to the height model representation one can summarize following results: branch 2 of the ADE models corresponds to the dilute loops with $n = 2\cos\left(\frac{\pi}{h}\right)$ and branch 1 is the dense phase of tri-critical models with $n = 2\cos\left(\frac{\pi}{h}\right)$. The results for some of the simple cases are as follows:

branch 2:	A_2 = critical percolation,	$c = 0$	$n = 1$,
branch 1:	A_2 = critical Ising	$c = 1/2$	$n = 1$,
branch 2:	A_3 = critical Ising	$c = 1/2$	$n = \sqrt{2}$,
branch 1:	A_3 = tri-critical Ising	$c = 7/10$	$n = \sqrt{2}$,
branch 2:	A_4 = tri-critical Ising	$c = 7/10$	$n = 2\cos\left(\frac{\pi}{5}\right)$,
branch 2:	D_4 = critical three-state Potts	$c = 4/5$	$n = \sqrt{3}$,
branch 1:	D_4 = tri-critical three-state Potts	$c = 6/7$	$n = \sqrt{3}$.

Using the above method it is easy to find the lattice realization for most of the proposed loop models, and the results are interestingly consistent. Following the same method it is possible to extract the loop models corresponding to minimal CFTs. However, the loop model for the non-diagonal cases with $g - h = -1$ is not extractable with this method because we are not able to find the dense phase of loop models for these cases. It seems that the dense lattice height model has not been proposed for this case.

One can summarize the important observations in the case of minimal models as follows: consider the operators $\phi_{1,2}$ and $\phi_{2,1}$ both the bulk and boundary cases. The highest eigenvalue of the fusion matrices of these operators in the bulk and on the boundary are the same and can define a loop model with fugacity n. One should note that in the corresponding loop model putting the operators $\phi_{1,2}$ and $\phi_{2,1}$ on the boundary just means that there is one critical curve emerging from the boundary similar as SLE with the fractal properties similar to the corresponding loop model in the bulk. The bulk operators $\phi_{1,2}$ and $\phi_{2,1}$ do not have obvious meaning with respect to the loop model but still they can give right answer for the fractal properties of the loop model. For example, the bulk $\phi_{1,2}$ after approaching the boundary is similar to $\phi_{1,3}$. This operator $\phi_{1,3}$ gives the fractal dimension D_b of the contact set of a loop

with boundary $D_b = 2 - 2h_{1,3}$. This is obvious also from the context of boundary operators, just we need to look at $\phi_{1,2}(x_1)$ and $\phi_{1,2}(x_2)$ in the limit of small $x_2 - x_1$. Then by fusion we have the operator $\phi_{1,3}$ on the boundary[4]. To find the fractal dimension of the loops in the bulk one needs to consider $\phi_{1,0}$ or $\phi_{0,1}$ then the fractal dimension is $D = 2 - 2h_{0,1}(h_{1,0})$. These operators are not in the Kac table and so one should look at them from the more general point of views such as the Coulomb gas methods.

To conclude this subsection, we proposed some loop representations for the minimal CFTs by using fusion of boundary operators. Then since ADE models give a lattice statistical model representation for minimal CFTs we used these models to extract physical loop models corresponding to ADE models. The fractal properties of these lattice loop models are the same as the loop models that we proposed by using the fusion of primary operators.

4.6. $SU_k(2)$ models

It is possible to follow the same calculation for every unitary minimal model. For example, for WZW $SU_k(2)$ models the classification of modular invariant partition functions is based on A–D–E–T graphs with $g = k+2$. The same method as the minimal models is applicable here and one can find boundary operators $\hat{\phi}_j$ with $1 \leqslant j \leqslant k+1$. The loop models have weights $d_j = \frac{\sin(\frac{\pi j}{g})}{\sin(\frac{\pi}{g})}$. Only $j = \frac{1}{2}$ has critical loop representation with the following loop weight:

$$n = 2\cos\left(\frac{\pi}{k+2}\right), \tag{4.14}$$

with $\kappa = 4\frac{k+2}{k+3}$ and $\kappa = 4\frac{k+2}{k+1}$ for the dilute and dense phases, respectively. The other loop models are not critical except for $k = 4$ with $n = 2$. The fusion graphs of the operators with $j \neq \frac{1}{2}$ are not decomposable to the simple graphs, however, the non-largest eigenvalues can be still relevant. For example, take $k = 5$ with $j = 3/2$, the fusion graph is similar to the one part of the ϕ_{31}'s fusion graph of the tri-critical three-state Potts model, the right one in figure A1. The eigenvalues are $\pm\frac{\sin(\frac{3\pi}{7})}{\sin(\frac{\pi}{7})}$, $\pm\frac{\sin(\frac{2\pi}{7})}{\sin(\frac{\pi}{7})}$ and $\pm\frac{\sin(\frac{\pi}{7})}{\sin(\frac{2\pi}{7})}$, the last two cases have critical loop representations. The similarities between fusion graphs of $SU_k(2)$ models with minimal models are not just an accident, they are based on the coset construction of the minimal models.

5. Discussion

We proposed a method to classify some possible loop models consistent with the conformal boundary conditions for generic rational CFT: take the simply laced classification of the corresponding minimal CFT then find the boundary operators and also the fusion matrices. Make the $O(n)$ loop model of the primary operator by the method that we discussed in section 3 and [4]. We think that there should be some connections between these loop models and the SLE interpretation of CFT investigated in [30] which is based on the connection of SLE with the null vectors in the CFT. This connection is not complete even for minimal CFTs because we do not know how to explain the boundary operators with the same loop model but with the different null vectors. For example, in the three-state Potts model ϵ, σ and $\sigma^\dagger$ are in the same sector from the boundary CFT point of view but just ϵ and σ have the required second level null vectors. However, from the null vector point of view this correspondence is not clear but it is possible to show that in the partition function level this similarity is more known.

[4] One should note that one can also give different fugacities for those loops that touch the boundary in the appropriate way and still preserve the conformal symmetry[7]. In our argument, we considered the $O(n)$ models that the fugacity is similar for the loops in the bulk and those that touch the boundary.

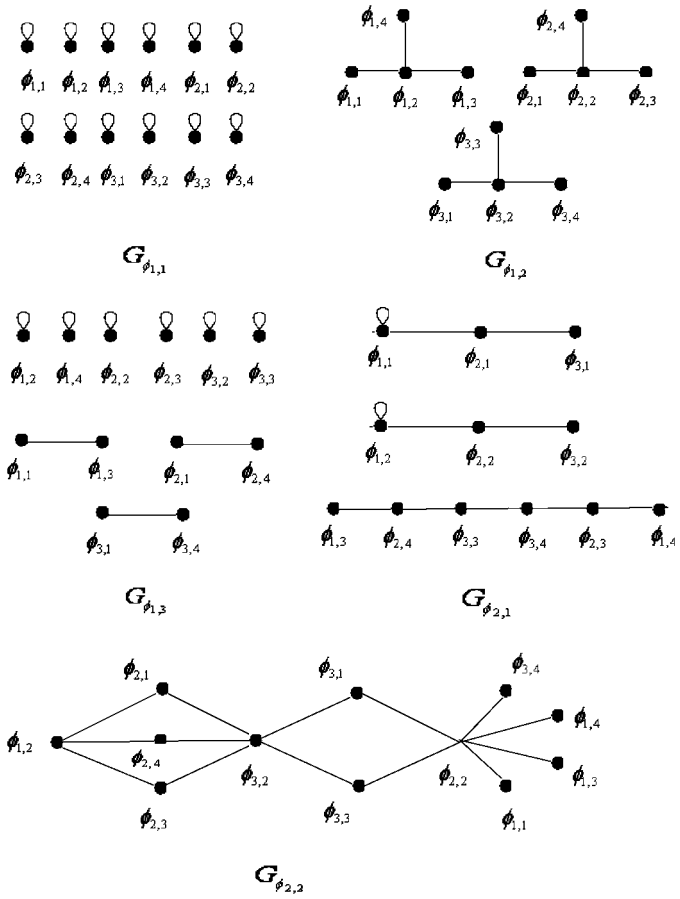

Figure A1. The fusion graphs of the tri-critical three-state Potts model.

Another way to look at the results of this paper is by conjecturing the largest eigenvalue of the fusion graph as the possible loop weight for the loop model in the universality class of the corresponding CFT without defining any height model on the fusion graph.

One possible generalization of the above construction is by considering graphs with largest eigenvalue greater than 2 as an adjacency graph of fused RSOS models and then extracting the loop model by the method investigated in [18]. The other interesting direction is to investigate the modular invariant partition functions of loop models and their possible connections to the classified modular invariant partition functions of minimal models; this is based on the direct investigation of the connection of our method to the classification of [6, 7].

Acknowledgments

I thank Roberto Tateo for useful discussions and Paul Fendley for useful comments. I also thank John Cardy for his useful criticism.

Appendix

In this appendix, we list the fusion graphs of the boundary operators in the tri-critical three-state Potts model. The fusion graphs are given in figure A1. The fusion graph

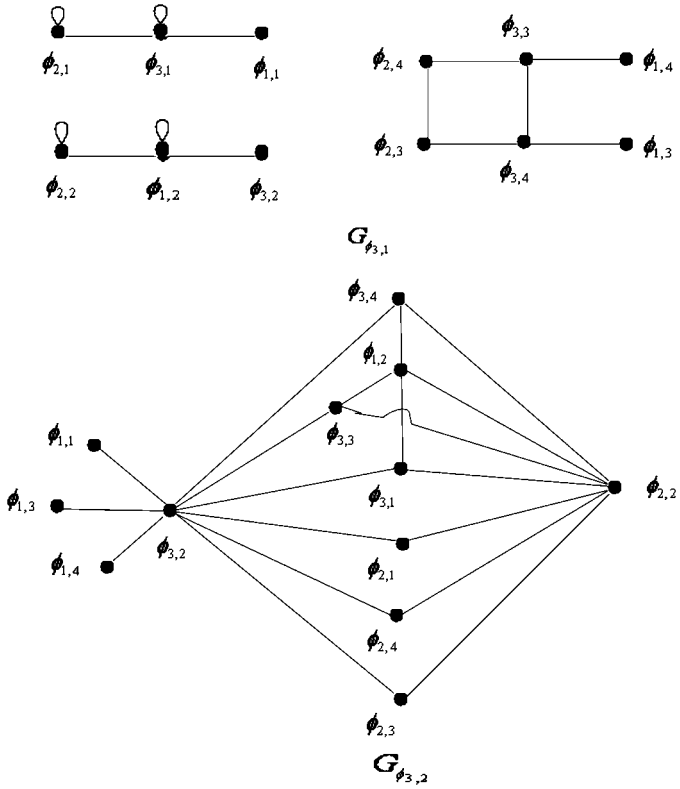

Figure A1. (Continued.)

of $\phi_{1,4}$ can be derived from the fusion graph of the operator $\phi_{1,3}$ by the following transformations:

$$\phi_{1,3} \leftrightarrow \phi_{1,4}, \qquad \phi_{2,3} \leftrightarrow \phi_{2,4}, \qquad \phi_{3,4} \leftrightarrow \phi_{3,3}. \tag{A.1}$$

The fusion graph of $\phi_{2,3}$ can be derived from the fusion graph of the operator $\phi_{2,1}$ by the following transformations:

$$\phi_{1,3} \leftrightarrow \phi_{1,1}, \qquad \phi_{2,3} \leftrightarrow \phi_{2,1}, \qquad \phi_{3,3} \leftrightarrow \phi_{3,1}. \tag{A.2}$$

Finally, the fusion graph of $\phi_{2,4}$ can be derived from the fusion graph of the operator $\phi_{2,1}$ by the following transformations:

$$\phi_{1,4} \leftrightarrow \phi_{1,1}, \qquad \phi_{2,4} \leftrightarrow \phi_{2,1}, \qquad \phi_{3,4} \leftrightarrow \phi_{3,1}. \tag{A.3}$$

To get the fusion graphs of $\phi_{3,3}$ and $\phi_{3,4}$ from the fusion graph of $\phi_{3,1}$ one just needs to use transformations (A.2) and (A.3), respectively.

We shall call the part of the fusion graph of $\phi_{3,1}$ with two neighbor blobs T_3^2, the lower index is the number of nodes and the upper index is the number of blobs attached to the neighboring nodes of the graphs starting from one of the extremes. These kinds of fusion graphs appear also in the fusion graph of $\phi_{j=1}$ of $SU_2(k)$ models.

References

[1] Nienhuis B 1984 *J. Stat. Phys.* **34** 731–61
[2] Freedmann M 2003 *Commun. Math. Phys.* **234** 129 (arXiv:quant-ph/0110060)
Freemann M, Nayak C and Shetengel K 2005 *Phys. Rev. Lett.* **94** 147205 (arXiv:cond-mat/0408257)
[3] Schramm O 2000 *Israel J. Math.* **118** 221 (arXiv:math.PR/9904022)
[4] Rajabpour M A 2008 *J. Phys. A: Math. Theor.* **41** 405001 (arXiv:0806.4520)
[5] Pasquier V 1986 *Nucl. Phys.* B **285** 162
Pasquier V 1987 *J. Phys. A: Math. Gen.* **20** L1229
Pasquier V 1987 *J. Phys. A: Math. Gen.* **20** 5707–17
[6] Jacobsen J L and Saleur H 2008 *Nucl. Phys.* B **788** 137–66 (arXiv:math-ph/0611078)
[7] Dubail J, Jacobsen J L and Saleur H 2009 *Nucl. Phys.* B **813** 430 (arXiv:0812.2746)
[8] Dubail J, Jacobsen J L and Saleur H (arXiv:0905.1382)
[9] Cardy J 2006 *J. Stat. Phys.* **125** 1 (arXiv:cond-mat/0604043)
[10] Cappelli A, Itzykson C and Zuber J-B 1987 *Commun. Math. Phys.* **113** 1
[11] Andrews G E, Baxter R J and Forrester P J 1984 *J. Stat. Phys.* **35** 193
Forrester P J and Baxter R J 1985 *J. Stat. Phys.* **38** 435
Pasquier V 1987 *Nucl. Phys.* B **285** 162
[12] Roche P 1992 *Phys. Lett.* B **285** 49–53
[13] Warnaar S O and Nienhuis B 1993 *J. Phys. A: Math. Gen.* **26** 2301–16
[14] Cardy J L 1989 *Nucl. Phys.* B **324** 581
[15] Behrend R E, Pearce P A and Zuber J B 1998 *J. Phys. A: Math. Gen.* **31** L763–70
Behrend R, Pearce P, Petkova V and Zuber J-B 1998 *Phys. Lett.* B **444** 163–6
[16] Behrend R, Pearce P, Petkova V and Zuber J-B 2000 *Nucl. Phys.* B **570** 525–89
Behrend R, Pearce P, Petkova V and Zuber J-B 2000 *Nucl. Phys.* B **579** 707–73
[17] Nienhuis B 1982 *Phys. Rev. Lett.* **49** 1062–5
[18] Fendley P 2006 *J. Phys. A: Math. Gen.* **39** 15445 (arXiv:cond-mat/0609435)
[19] Fendley P and Jacobsen J L 2008 *J. Phys. A: Math. Theor.* **41** 215001 (arXiv:0803.2618)
[20] Chim L 1996 *Int. J. Mod. Phys.* A **11** 4491 (arXiv:hep-th/9510008)
Nepomechie R I 2001 *J. Phys. A: Math. Gen.* **34** 6509–24 (arXiv:hep-th/0102010)
[21] Fendley P and Ginsparg P 1989 *Nucl. Phys.* B **324** 549–80
[22] Deng Y, Blöte H W J and Nienhuis B 2004 *Phys. Rev.* E **69** 026123
[23] Deng Y, Guo W and Blöte H W J 2005 *Phys. Rev.* E **72** 016101
[24] Affleck I, Oshikawa M and Saleur H 1998 *J. Phys. A: Math. Gen.* **31** 5827–42 (arXiv:cond-mat/9804117)
[25] Gamsa A and Cardy J 2007 *J. Stat. Mech.* P08020 (arXiv:0705.1510)
[26] Cardy J 2007 *J. Phys. A: Math. Theor.* **40** 1427–38 (arXiv:math-ph/0610030)
[27] Blöte H W J and Nienhuis B 1989 *J. Phys. A: Math. Gen.* **22** 1415–38
[28] Schramm O, Sheffield S and Wilson D B (arXiv:math/0611687)
[29] Warnaar S O, Nienhuis B and Seaton K A 1992 *Phys. Rev. Lett.* **69** 710–2
[30] Bauer M and Bernard D 2002 *Phys. Lett.* B **543** 135–8 (arXiv:math-ph/0206028)
Friedrich R and Werner W 2002 *C. R. Math.* **335** 947–52 (arXiv:math/0209382)
Bettelheim E, Gruzberg I A, Ludwig A W W and Wiegmann P 2005 *Phys. Rev. Lett.* **95** 251601 (arXiv:hep-th/0503013)
[31] Ikhlef Y and Cardy J 2009 *J. Phys. A: Math. Theor.* **42** 102001 (arXiv:0810.5037)